ARTICLE

Fabrication of TiB_2/Al composite by melt-SHS process with different content of titanium powder

He Li, Lihua Chai, Haijing Wang, Ziyong Chen,[a)] Guodong Shi, Zhilei Xiang, and Tounan Jin
College of Materials Science and Engineering, Beijing University of Technology, Chaoyang District, Beijing 100122, China

Melt-SHS (self-propagating high-temperature synthesis), based on the SHS process and oxide reaction method, was used for preparation of TiB_2/Al composites. The mass ratio of two reactants, Ti powder/TiO_2, in initial powder mixture was varied from 0:1 to 1:0. The results showed that the 5 wt% TiB_2/Al composites could be successfully produced by a reaction of aluminum powder, TiO_2, and B_2O_3 in Al melt at 950 °C, while the reaction rate was slow. The addition of titanium powder helps to reduce the content of Al_2O_3 and destroy the coating structure of Al_2O_3 covered TiB_2 particles, which leads to the acceleration of reaction process and improvement of particle concentration. A significant improvement was that TiB_2 particles were dispersively distributed when the mass ratio of Ti powder/TiO_2 was 2:3. As a result, the 5 wt% TiB_2/Al composites fabricated by melt-SHS process with modified reactants ratio showed excellent tensile properties with the ultimate tensile strength as high as 114.24 MPa. Besides, the composite also showed superior ductility.

I. INTRODUCTION

In situ particulate reinforced aluminum matrix composites (Al MMCs) are widely used in the aerospace and automotive industries due to their excellent properties, such as high specific strength, low weight, and chemical inertness.[1] It consists of matrix and the reinforcement, and the reinforcement is one of the most important parts. TiB_2 particles reinforced Al MMCs is one of the most widely used particulate reinforced Al MMCs because of its outstanding properties, such as low density, high melting point, high elastic modulus, and good lattice matching relations with the aluminum matrix.[2]

It has been reported in many studies that TiB_2 particles can be synthesized by *in situ* synthesis method, and the process offers significant advantages over the conventional processing from both technical and economic standpoints,[2,3] such as its excellent interfacial compatibility between matrices and reinforcements, thermodynamically stable, and distribution uniformity of the reinforcements in the matrix.

In situ TiB_2 particles reinforced aluminum matrix composites can be synthesized by the salt-metal reaction, self-propagating high-temperature synthesis (SHS), hot pressing, pressureless sintering, and mechanochemical synthesis.[3,4] The salt-metal reaction is the most commonly used *in situ* methods.[5] In this processing, the mixed K_2TiF_6 and KBF_4 were used as reactants, which reacted with molten Al at a high temperature to form TiB_2 particles in the Al matrix.[6] However, the method has fluoride emissions and the dross needs to be disposed. As one of the fabrication techniques to synthesize *in situ* ceramic particulate reinforced MMCs, SHS technology has received much attention because of its low energy consumption and high product purity. Nevertheless, the price of the reactants is expensive, and procedure is complicated and time consuming because the final products are porous and need to combine with a densification step; the react temperature cannot be controlled easily as well. To decrease the cost of reactants, Al–TiO_2–B,[7] TiO_2–B_4C–C,[8] Al–Ti–B,[9,10] Al–TiO_2–B_2O_3–Na_3AlF_6,[11] and Al–TiO_2–B_2O_3[12] systems were studied to fabricate TiB_2 particles reinforced aluminum matrix composites. Due to the high price of the elemental powder, the oxide and compounds of titanium and boron were popular as reactants in the new system. However, another main product, Al_2O_3, needs to be cleared, and this undoubtedly leads the amount of reactants and reaction process to be more difficult to control.

In this study, a modified method melt-SHS process which combined the advantages of low price of oxide reactant and SHS process was used to synthesize Al/TiB_2 composites. Furthermore, the melt-SHS method is environmentally friendly due to the clean products. The reactants, H_3BO_3, TiO_2, Al powder, and Ti powder, were used in the process since Ti powder could be used as a reductant and a combustion promoter. To confirm the optimum reactant ratio and produce the low-cost and

efficient composites, the different ratios of H_3BO_3, TiO_2, and Ti powder were applied.

II. EXPERIMENTAL PROCEDURE

A. Raw materials

High purity aluminum (>99.9 wt%) was used as the base metal. Two kinds of chemical powders, namely TiO_2 (200 mesh) and H_3BO_3 (200 mesh), and two types of metal powders, namely Al powder (300 mesh) and Ti powder (300 mesh), were used to synthesize the TiB_2 particles.

B. Processing

With the atomic ratio Ti/4B, TiO_2 and H_3BO_3 were first dried at 200 °C for 2 h, and then a percentage of aluminum and titanium powder were added in the mixed powder and mechanical stirred homogeneously. The final mixed powder was pressed into a cylinder ($\varphi 62.5 \times 12$ mm^3) to make a powder block. After that, Al ingot was melted in a graphite crucible resistance furnace as the temperature reached 950 °C, which was measured by a thermocouple, then the prepared powder block was pressed into the melt. Melt-SHS reaction between the powder cylinder and the molten Al to form TiB_2 particles. The whole preparation process is shown in Fig. 1, and the synthesis process is in the air. Two times were marked: one is the response time t_1 which is the time from the cylinder touched aluminum melt to the emergence of the spark. The other is the reaction time denoted as t_2, which indicates the time from the emergence of the spark until the spark went out. After the reaction, the melt was mechanically stirred for 10 min, the reaction holding time was set as 30 min at 800 °C, and finally the melt was poured into a steel mold ($\varphi 95 \times 150$ mm^3) at 720 °C. Then the TiB_2/Al composite billets were extruded into bar composites with an extrusion ratio of 25:1 at about 400 °C. The four composites correspond to the four quality ratio of

Ti powder/TiO_2 in the initial powder mixture which varied from 0:1 to 1:0 (showed in Table I).

The mechanical properties were evaluated by the tensile test, which was carried out on a computerized universal testing machine at a velocity of 0.05 mm/s. Three tests were conducted for each composite to get a precise value for each property.

C. Characterization

The metallographic specimens were intercepted from each bottom of the samples. X-ray diffraction (D8 ADVANCE, Bruker, Karlsruhe, Germany) was used to analyse the diffraction phases in the composite. Scanning electron microscopy (QUANTA200, FEI Company, Hillsboro, Oregon) equipped with an energy-dispersive X-ray spectroscopy (EDS) was used to observe the morphology and distribution of particles in the composites. Besides, the software Image-Pro plus 6 (Media Cybernetics, Rockville, Maryland) was used to statistically analyze the particle size distribution.

III. RESULTS AND DISCUSSION

A. Thermodynamic analysis

Before the preparation of powder block, TiO_2 and H_3BO_3 mixture was dried to remove the water in boric

TABLE I. Particulate material additions for the production of 5 wt% TiB_2/Al composites.

Composite	Composite component (wt%)	Source of B	Source of Ti	Mass ratio of Ti powder/TiO_2
1#	Al–5TiB_2	H_3BO_3	TiO_2	0:1
2#	Al–5TiB_2	H_3BO_3	Ti powder + TiO_2	2:3
3#	Al–5TiB_2	H_3BO_3	Ti powder + TiO_2	1:1
4#	Al–5TiB_2	H_3BO_3	Ti powder	1:0
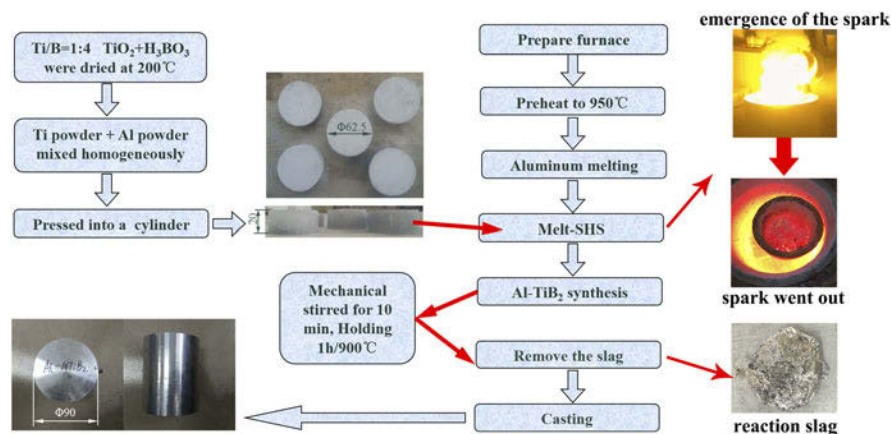
FIG. 1. The whole preparation process.
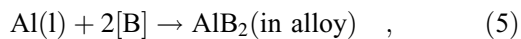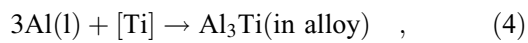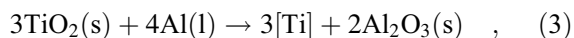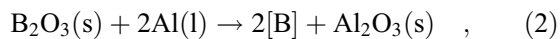
acid. It was easier to produce crystalline lumps since boric acid was dried separately. The reaction of the dehydration process can be written as function (1),

$$2H_3BO_3(s) \rightarrow 3H_2O(g) + B_2O_3(s) \quad . \qquad (1)$$
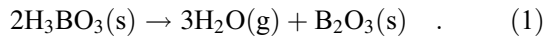
The formation of ceramic particles via melt-SHS process is a thermodynamically chemical reaction. The possible reaction basically has the following several parts: (i) at a predetermined temperature, Al powder produces sparks as an igniter composition, and the combustion wave diffuses along the powder cylinder. (ii) The aluminothermy reduction of B_2O_3 and TiO_2 at the molten flux-liquid metal interface forms B, Ti atoms, and Al_2O_3, which can be written as Eqs. (2) and (3). (iii) The formation of Al_3Ti, AlB_2, and TiB_2 by combination reaction of B, Ti, and Al. The reactions are shown in Eqs. (4), (5), and (7). (iv) The boron atoms react with Al_3Ti and generate TiB_2. The last part reaction is exhibited as Eq. (6),

$$B_2O_3(s) + 2Al(l) \rightarrow 2[B] + Al_2O_3(s) \quad , \qquad (2)$$

$$3TiO_2(s) + 4Al(l) \rightarrow 3[Ti] + 2Al_2O_3(s) \quad , \qquad (3)$$

$$3Al(l) + [Ti] \rightarrow Al_3Ti(\text{in alloy}) \quad , \qquad (4)$$

$$Al(l) + 2[B] \rightarrow AlB_2(\text{in alloy}) \quad , \qquad (5)$$

$$Al_3Ti(\text{in alloy}) + 2[B] \rightarrow 3[Al] + TiB_2(\text{in alloy}) \quad , \qquad (6)$$

$$[Ti] + 2[B] \rightarrow TiB_2(\text{in alloy}) \quad . \qquad (7)$$
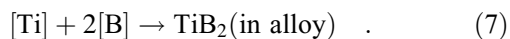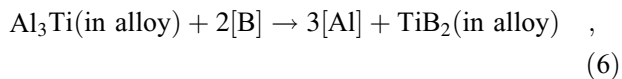
The temperature dependence of the reaction enthalpy (ΔH_T) and free energy (ΔG_T) changes for these six reactions are summarized in Fig. 2. The results indicate that the values of ΔH_T and ΔG_T in all functions are negative, and further illustrate that the reactions are exothermic reactions and can proceed spontaneously. The lower the ΔG_T is, the higher possibility the reaction goes.

It is easy to observe that Eq. (7) has the greatest possibility over other functions in the parts (iii) and (iv), and TiB_2 particle is the most stable phase. A notable finding is that the TiB_2 is the main product, and $TiAl_3$ and AlB_2 are much less competitive due to the higher ΔG_T.

The SHS reaction maintains by the heat released in the process of the reaction. It is necessary to analyse the thermodynamics which enables a SHS reaction to proceed successfully. For the SHS reaction, an experience criterion was put forward; when $T_{ad} \geq 1527\ °C$, the SHS reaction sustains itself, otherwise needs supplement system energy.[13] The adiabatic temperature can be calculated according to the materials formed in the process of reaction and enthalpy of phase changes. The overall reaction showing the formation of TiB_2 can be written as

$$10Al + 3TiO_2 + 3B_2O_3 = 5Al_2O_3 + 3TiB_2 \quad . \qquad (8)$$
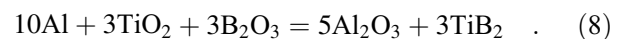
According to the first law of thermodynamics,

$$C_p = \frac{dH}{dT} \quad .$$

The former equation at the interval of room temperature and temperature T is integrated, and the solid phase transformation and melting phenomenon of the material within the scope of the studied temperature T range are considered. Ignoring the vaporization phenomenon, the equation is as follows:

$$H_T^\Theta - H_{298}^\Theta = \int_{298}^{T_{tr}} C_{p,m}dT + \Delta H_{tr} + \int_{T_{tr}}^{T_m} C'_{p,m}dT$$
$$+ \Delta H_m + \int_{T_m}^{T} C''_{p,m}dT \quad ,$$

$$C_p = a + b \times 10^{-3}T + c \times 10^{5}T^{-2} + d \times 10^{-6}T^2$$
$$+ e \times 10^{8}T^{-3} \quad .$$

$C_{p,m}$, $C'_{p,m}$, and $C''_{p,m}$ are the molar constant pressure heat capacity of substance, J/(mol K). $H_T^\Theta - H_{298}^\Theta$ is the
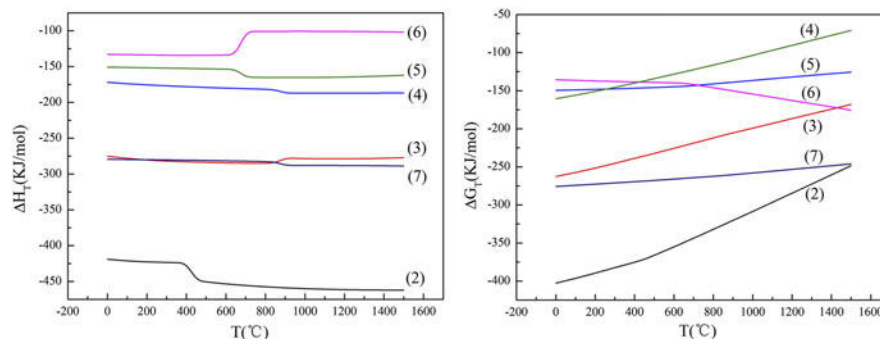

FIG. 2. Relationship between the temperature and the reaction enthalpy (ΔH_T) and free energy (ΔG_T) change for these six reactions.

relative material mole enthalpy, J/mol. T_{tr} and T_m are the phase transition temperature and melting point of material, K. ΔH_{tr} and ΔH_m are the solid phase transformation and melting heat of material, J/mol.

According to the Kirchhoff equation,

$$d\Delta H_T^{\ominus} = \Delta C_p dT \quad .$$

In the equation, ΔC_p is the D-value between the sum isobaric heat capacity of products and reactants, namely, the heat capacity difference,

$$\Delta C_p = \sum \left(n_i C_{p,i}\right)_{product} - \sum \left(n_i C_{p,i}\right)_{reactant} \quad .$$

In the equation, n_i is the mole of reactants participate in the reaction and C_p is the molar constant pressure heat capacity.

Assuming that the reactants are involved in the reaction completely under the condition of adiabatic temperature, the release of heat will be all applied to the reaction. If the reaction proceeds at room temperature (298 K), the equation is as follows:

$$\Delta H_{298}^{\ominus} + \sum n_i \left(H_T^{\ominus} + H_{298}^{\ominus}\right)_{i,product} = 0 \quad .$$

$\Delta H_{298}^{\ominus}$ is the heating effect of the reaction at room temperature. If the reactants are preheated at T_0,

$$\sum n_i \left(H_{298}^{\ominus} + H_{T_0}^{\ominus}\right)_{i,reactant} + \sum n_i \left(H_T^{\ominus} + H_{298}^{\ominus}\right)_{i,product} + \Delta H_{298}^{\ominus} = 0 \quad .$$

If the adiabatic temperature of reaction is 1527 °C, preheat temperature T_0 is easily figured out. After calculation, the T_0 is 892 °C. Considering that the experiment is under atmospheric conditions, to ensure the smooth progress of the reaction, the starting reaction temperature of 950 °C was used.

B. X-ray diffractions analysis

XRD patterns of the four composites and the reaction slag are shown in Fig. 3. The presence of TiB$_2$ peaks and TiAl$_3$ peaks in the 1#, 2#, and 3# composites [Fig. 3(a)] confirms the formation of TiB$_2$ and TiAl$_3$. The TiB$_2$ peaks in 4# composite are not obvious. XRD patterns of the reaction slag [Fig. 3(b)] confirm the formation of TiB$_2$ and Al$_2$O$_3$ in the fabrication of four composites. It can be seen that the 4# slag has more obvious peaks of TiB$_2$ and Al$_2$O$_3$, which means that TiB$_2$ particles which failed to spread to aluminum melt mainly exist in the slag. It is interesting to note that there are no obvious peaks of AlB$_2$ and Al$_2$O$_3$ in the spectra of the TiB$_2$/Al composites, while Al$_2$O$_3$ mainly exists in the reaction slag which had been cleared out of the Al melt.

C. Microstructures of reaction slag

To make sure TiB$_2$ and Al$_2$O$_3$ particles exist in the reaction slag, microstructures and energy spectrum analysis of the slag are shown in Fig. 4. Combining XRD and energy spectrum analysis [Figs. 4(c) and 4(d)], accumulation area of Al$_2$O$_3$ [Fig. 4(a)] and TiB$_2$ [Fig. 4(b)] was found in the slag. It can be concluded that Al$_2$O$_3$ particles were taken away with the reaction slag, and there was still a percentage of TiB$_2$ particles that have not been able to diffuse into the Al melt. This is mainly because the Al$_2$O$_3$ particles gathered in the block after the reaction. Besides, the initial size of TiB$_2$ particles formatted in the block were much less than the holes in the block, which results in the smaller size TiB$_2$ particles diffused to the aluminum melt easily at the end of the reaction. With the increase of the reaction holding time, part of TiB$_2$
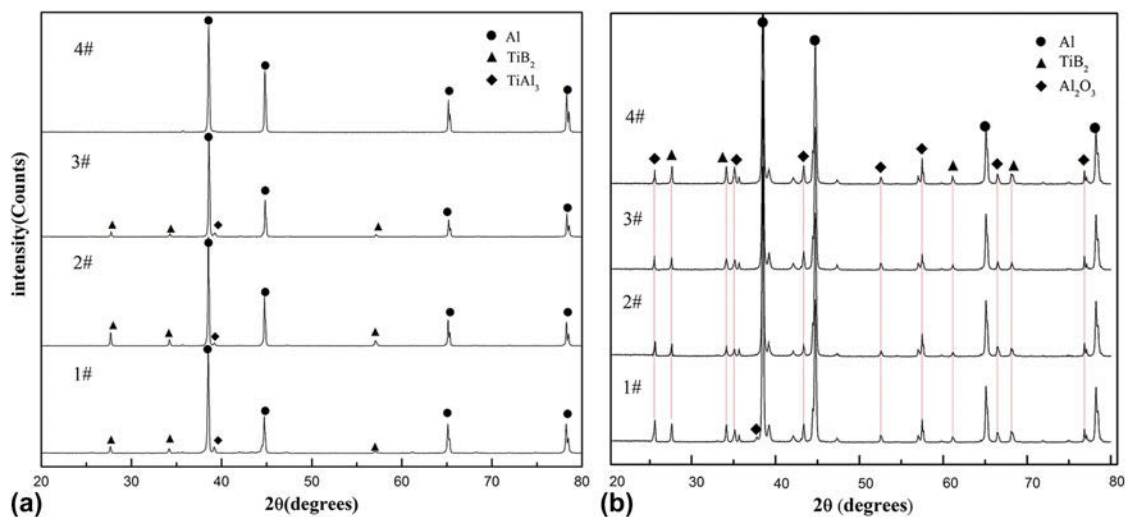

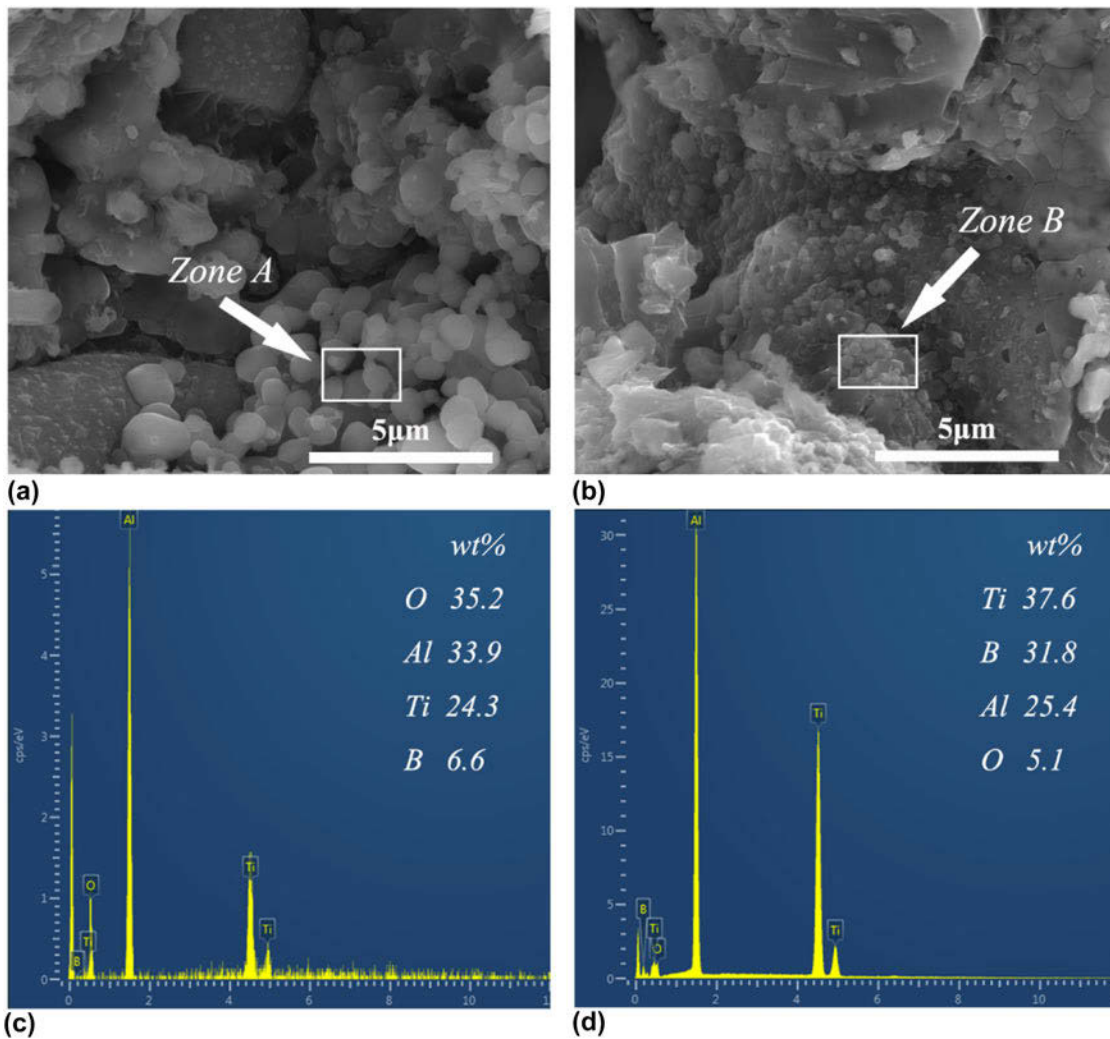FIG. 3. XRD spectra of (a) 5% TiB$_2$/Al composites and (b) reaction slag.

FIG. 4. Microstructures and energy spectrum analysis of 1# composite reaction slag: (a) accumulation area of Al$_2$O$_3$, (b) accumulation area of TiB$_2$, (c) energy spectrum analysis of Zone A, and (d) energy spectrum analysis of Zone B.

particles in the block grew up to a bigger size and stayed in the melt.

D. Microstructure and properties of composites

Microstructures and the particle size distribution of four composites with different mass ratios of Ti powder/TiO$_2$ in raw materials are showed in Fig. 5. And the mechanical properties of 5 wt% TiB$_2$/Al composites were shown in Table II.

According to XRD [Fig. 3(a)] and EDS analysis [Fig. 5(e)], it can be confirmed that the white particles are TiB$_2$. The morphology of TiB$_2$ particles in composite 1# [Fig. 5(a)] presents the hexagonal shape, and the average size is nearly 0.91 μm [Fig. 5(f)]. Compared to composite 1#, composite 2# [Fig. 5(b)], which has additional Ti powder in raw materials mixture and with a mass ratio of Ti powder/TiO$_2$ of 2:3, exhibits a uniform distribution of TiB$_2$ particles in the Al matrix, the average

size is nearly 0.67 μm [Fig. 5(f)], and the contents of TiB$_2$ particles increased. It is seen that when Ti powder was added into the powder block, the assimilation of B increased and showed an increase in the number of the TiB$_2$ particles. Thus the 2# composite showed excellent tensile properties: the ultimate tensile strength (UTS) is up to 114.24 MPa, the hardness is 25.54 HB, and the elongation is 33.15% which is also a superior ductility. After the fast exothermic combustion reaction, the temperature in the combustion zone decreases sharply and the desired phases are vigorously formed in great numbers. With increasing of Ti powder mass ratio further, the contents of TiB$_2$ particles decrease as shown in Figs. 5(c) and 5(d), and the average size increases to 0.72 μm and 0.95 μm, respectively [Fig. 5(f)]. Besides, the distributions of TiB$_2$ particles were uneven when the quality ratio of Ti powder/TiO$_2$ was larger than 2:3 which resulted from the relatively higher adiabatic temperature induced by the
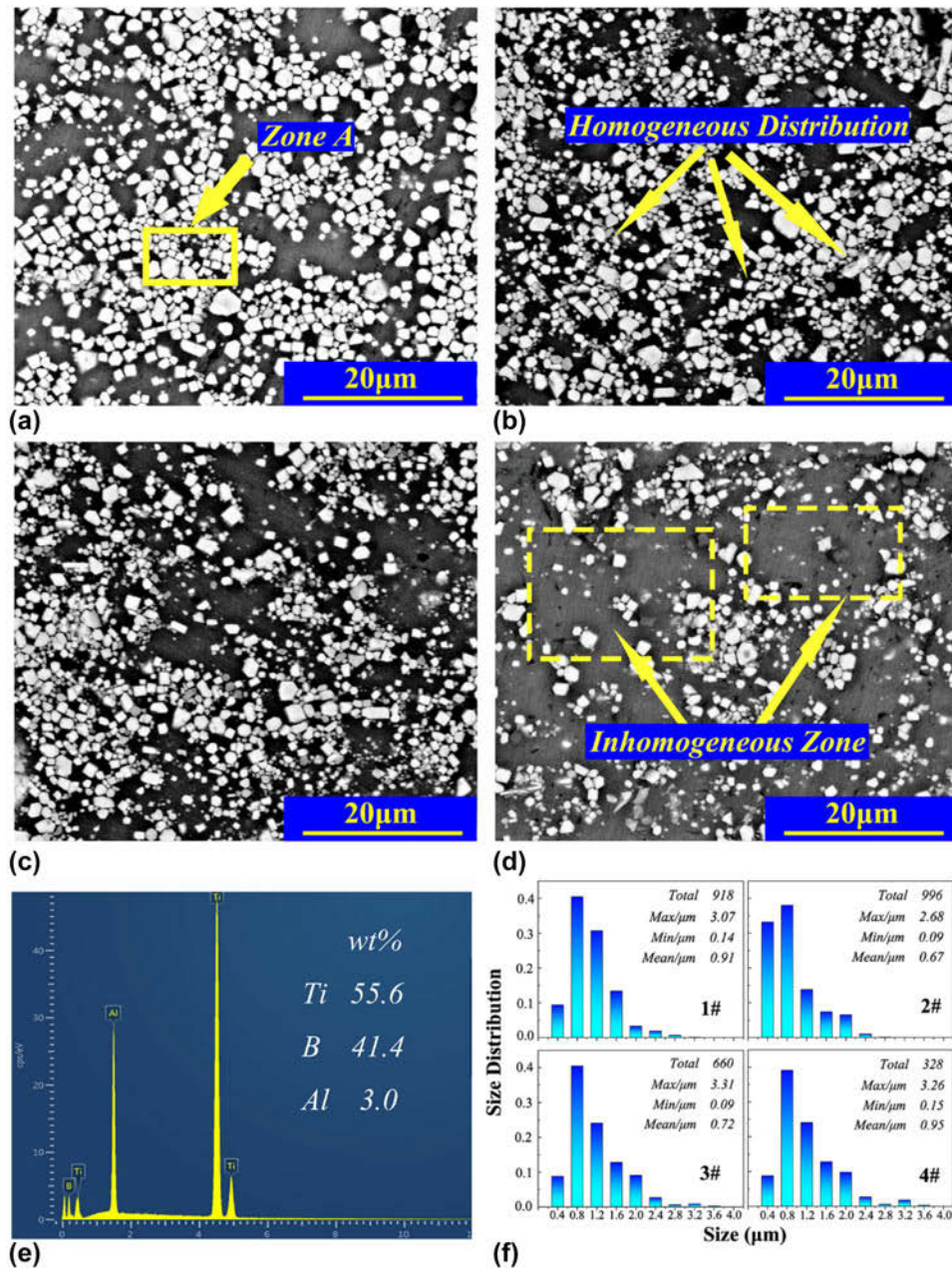
FIG. 5. Microstructures and particle size distribution of four composites with different quality ratio of Ti powder/TiO$_2$ in raw materials: (a) 1#, (b) 2#, (c) 3#, (d) 4#, (e) EDS analysis of Zone A, and (f) particle size distribution.

TABLE II. Mechanical properties of 5 wt% TiB$_2$/Al composites.

Sample no.	Hardness (HB)	UTS (MPa)	$\sigma_{0.2}$ (MPa)	Elongation (%)
1#	24.12	108.81	68.44	34.01
2#	25.54	114.24	74.56	33.15
3#	23.26	98.78	55.34	35.27
4#	20.78	82.15	47.39	37.66

addition of Ti powder. And the tensile properties were also not that good, which showed lower UTS, because high temperature led to a large amount of evaporation of aluminum melt and made the TiB$_2$ diffusion become more difficult. According to the data of XRD spectra and the microstructures, it was confirmed that the amount of TiAl$_3$ phase was too few to show in the microstructure. It may be because a long enough reaction holding time results in less available TiAl$_3$ in the melt, as a result of its continuing decomposition to form TiB$_2$.

E. *In situ* formation of TiB$_2$ particulates

The response time t_1 and the reaction time t_2 are showed in Table III.

After the powder block was put into an aluminum melt, the composite 1# did not spark immediately. Approximately 60 s later, the spark appeared and extinguished in 2 min. While the composites with the additions of Ti powder (the composite 2#, 3#, 4#) appeared the spark in 10 s and kept for 1 min until the reaction finished. The reactants of composite 1# are H$_3$BO$_3$ and TiO$_2$ which resulted in the products containing a mass of Al$_2$O$_3$. A mount of the reactants was forbidden to touch the Al melt because the powder cylinder was surrounded by the formed Al$_2$O$_3$ which could be deduced from the microstructure of the slag as shown in Figs. 6(a) and 6(b); thus, the reaction speed was reduced greatly. Majority of nanometer TiB$_2$ particles were trapped in the melt slag and could not spread out as shown in Fig. 6(c).

TABLE III. Composite reaction waiting time t_1 and the actual reaction time t_2.

Composite	1#	2#	3#	4#
t_1 (s)	40–60	5–10	5–10	5–10
t_2 (s)	100–130	30–60	20–50	10–30

According to the thermodynamic analysis and the microstructures, the reaction process analysis was described in Fig. 7. This reaction process used the heat released by the reaction to synthesise TiB$_2$/Al composites. When the mixed powder cylinder was pressed into the high temperature aluminum liquid, parts of titanium powder first ignition where the powder and liquid aluminum contact because of the flammable properties of titanium powder, and aluminum powder melted due to the low melting point. TiO$_2$ and B$_2$O$_3$ reacted with the molten aluminum to form free B atoms and Ti atoms. Since the Gibbs free energy of aluminum oxide is lower than that for boron oxide, chemical reactions occur at the interface between molten aluminum and boron oxide.[12,14] As boron atoms go into solution in the molten aluminum, aluminum oxide covers the top of melt as slag and formed a coating structure. The reaction released heat to melt the rest of the parts of solid titanium powder, but it only occurred in a few atomic layers of the Ti particles surface, and the molten titanium reacted with the free boron to produce TiB$_2$ particles. According to the thermodynamic analysis, it is easy to form AlB$_2$ and TiAl$_3$ phases, respectively, when the free B and Ti atoms
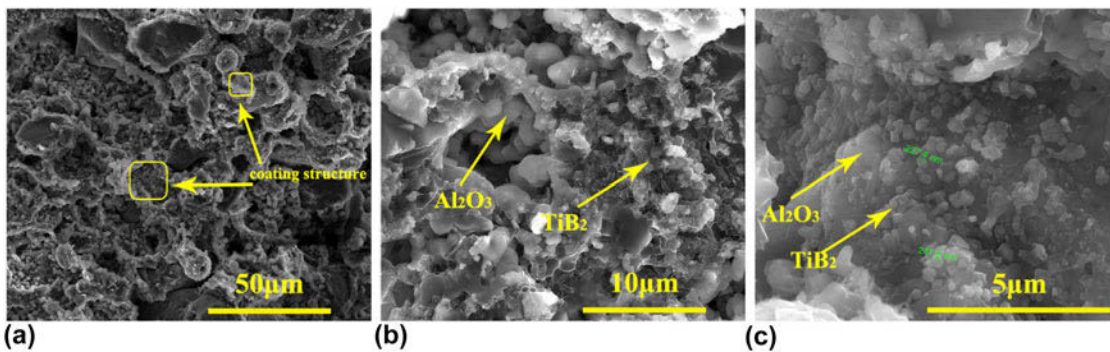

FIG. 6. Microstructure of reaction slag of 1# composite: (a) coating structure, (b) local amplification figure, and (c) nanometer TiB$_2$ particles in the slag.
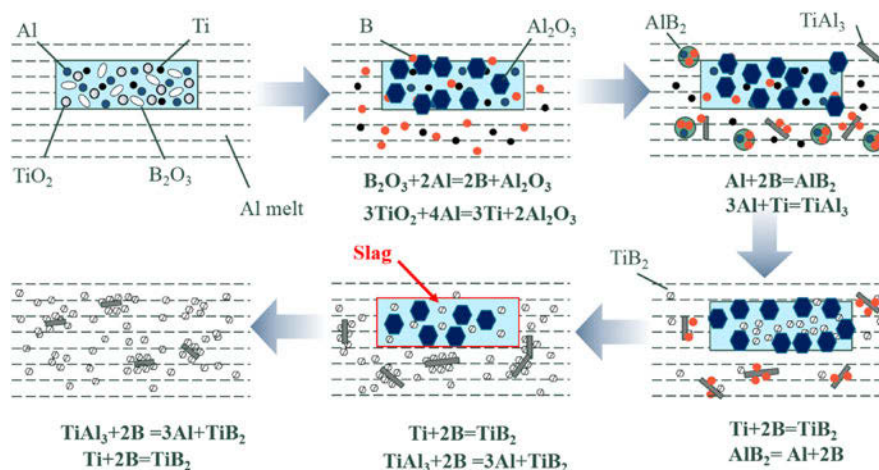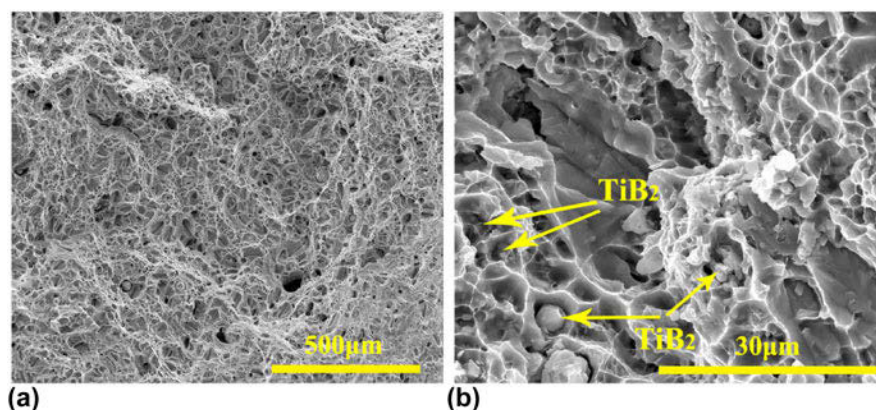

FIG. 7. Reaction process analysis.

FIG. 8. The fractographs of the composite fabricated by melt-SHS with the ratio of Ti powder TiO_2 as 2:3: (a) macroscopic fracture and (b) TiB_2 particles in the fracture.

met the molten Al. It has been reported[15,16] that the dominant bonding in TiB_2 is covalent, which leads to its great structural stability at high temperature and the dominant bonding in AlB_2 is ionic due to the large charge transfer from aluminum to boron. It means that AlB_2 phases were relatively unstable from the view of thermodynamics, and it would decompose back to Al and B atoms. The free B atoms not only combined with Ti atoms to form TiB_2 but also took part in the reduction reaction with $TiAl_3$ to form TiB_2. The Al_2O_3 particles were cleaned out of the Al melt with the reaction slag. It has been reported that the removal of Al_2O_3 promotes the particle wetting.[17] With the Al_2O_3 out of the melt, the wetting angle between the liquid Al and TiB_2 decreased, hence also producing a good interfacial integrity. The addition of titanium powder helps to reduce the content of Al_2O_3 and destroy the coating structure of Al_2O_3 covered TiB_2 particles, which lead to the acceleration of reaction process and improvement of particle concentration. Therefore, the addition of titanium powder could reduce the generation and accumulation of Al_2O_3 and proceed the reaction.

F. Fractograph

Figure 8 shows the fractographs of the composites fabricated by the melt-SHS with the ratio of Ti powder/ TiO_2 as 2:3 (2# composite) which has the high UTS of 114.24 MPa. As shown in Fig. 8(a), a large number of micron and deep equiaxed dimples dominate in the fracture of the matrix, which indicates that ductile fracture happened during tensile test. TiB_2 particles were discovered in the equiaxed dimples as shown in Fig. 8(b). It has been reported that TiB_2 particles act as effective barriers to the growth and coalescence of the voids which resulted in the matrix grain refinement.[18,19] Due to the great coherent relationship between TiB_2 particles and Al matrix, the good wetting, and the strong interface bonding, the composites achieved excellent tensile properties.

IV. CONCLUSIONS

Using the melt-SHS method, 5 wt% TiB_2/Al composites were prepared by the reaction of Al powder, Ti powder, TiO_2, and H_3BO_3 in Al melt successfully. The results are showed as follows:

(1) 5 wt% TiB_2/Al composite could be produced at 950 °C, but the reaction rate is slow when only adding TiO_2 as the main source of Ti. The addition of Ti powder into the powder block significantly reduces the response time from more than 40 s to less than 10 s and improves the reaction rate. With the increase of titanium powder in the raw powder materials, the reaction rate increased.

(2) Al_2O_3 particles mainly exist in the melt slag and can be cleared directly. The addition of titanium powder helps to reduce the content of Al_2O_3, destroy the coating structure of Al_2O_3 covered TiB_2 particles, speed up the reaction process, and improve particle concentration.

(3) The microstructure of composites mainly presents sub-micron TiB_2 particles, and the average size of the particles is 0.67 μm with Ti powder addition to the reactants and the optimized ratio of Ti powder/TiO_2 is 2:3. While the distribution of TiB_2 particles were heterogeneous and the particle size increased when the quality ratio of Ti powder/TiO_2 is larger than 2:3 which resulted from the relatively increased adiabatic temperature induced by the additions of Ti powder.

(4) The 5 wt% TiB_2/Al composite fabricated by melt-SHS process with modified reactants ratio showed excellent tensile properties with the UTS as high as 114.24 MPa, and the composite also showed superior ductility.

REFERENCES

1. Q. Zhang, W.H. Wu, G.Q. Chen, L.T. Jiang, and B.F. Luan: The thermal expansion and mechanical properties of high reinforcement content SiCp/Al composites fabricated by squeeze casting technology. *Composites, Part A* **34**, 1023–1027 (2003).
2. C.F. Feng and L. Froyen: Microstructures of *in situ* Al/TiB₂ MMCs prepared by acasting route. *J. Mater. Sci.* **35**, 837–850 (2000).

3. S. Kumar, V.S. Sarma, and B.S. Murty: A statistical analysis on erosion wear behavior of A356 alloy reinforced with *in situ* formed TiB$_2$ particles. *Mater. Sci. Eng., A* **476**, 333–340 (2008).

4. Z.W. Liu, M. Rakita, W. Xu, X.M. Wang, and Q.Y. Han: Ultrasound assisted salts-metal reaction for synthesizing TiB$_2$ particles at low temperature. *Chem. Eng. J.* **263**, 317–324 (2015).

5. Q. Gao, S.S. Wu, S.L. Lü, X.C.H. Duan, and P. An: Preparation of *in situ* 5 vol% TiB$_2$ particulate reinforced Al–4.5Cu alloy matrix composites assisted by improved mechanical stirring process. *Mater. Des.* **94**, 79–86 (2016).

6. S.C. Tjong and Z.Y. Ma: Microstructural and mechanical characteristics of *in situ* metal matrix composites. *Mater. Sci. Eng., R* **29**, 49–113 (2000).

7. C.F. Feng and L. Froyen: On the reaction kinetics of an Al–TiO$_2$–B system for producing *in situ* Al/(Al$_2$O$_3$ + TiB$_2$) composites. *J. Mater. Sci. Lett.* **19**, 103–105 (2000).

8. R. Koc and D.B. Hodge: Production of TiB$_2$ from a precursor containing carbon coated TiO$_2$ and B$_4$C. *J. Mater. Sci. Lett.* **19**, 667–669 (2000).

9. P.J. Li, E.G. Kandalova, V.I. Nikitin, A.R. Luts, A.G. Makarenko, and Y.F. Zhang: Effect of fluxes on structure formation of SHS Al–Ti–B grain refiner. *Mater. Lett.* **57**, 3694–3698 (2003).

10. V.I. Nikitin, W.Q. Jie, E.G. Kandalova, A.G. Makurenko, and L. Yong: Preparation of Al–Ti–B grain refiner by SHS technology. *Scr. Mater.* **42**, 561–566 (2000).

11. Y.F. Yang and Q.C. Jiang: Effect of TiB$_2$/TiC ratio on the microstructure and mechanical properties of high volume fractions of TiB$_2$/TiC reinforced Fe matrix composite. *Int. J. Refract. Met. Hard Mater.* **38**, 137–139 (2003).

12. E.M. Sharifi, F. Karimzadeh, and M.H. Enayati: Synthesis of titanium diboride reinforced alumina matrix nanocomposite by mechanochemical reaction of Al–TiO$_2$–B$_2$O$_3$. *J. Alloys Compd.* **502**, 508–512 (2010).

13. C.L. Yeh and S.H. Su: *In situ* formation of TiAl–TiB$_2$ composite by SHS. *J. Alloys Compd.* **407**, 150–156 (2006).

14. A. Changizi, A. Kalkanli, and N. Sevinc: Production of *in situ* aluminum–titanium diboride composite formed by slag–metal reaction. *J. Alloys Compd.* **509**, 237–240 (2011).

15. H.L. Zhang, Y.F. Han, J. Wang, Y.B. Dai, and B.D. Sun: An ab initio molecular dynamics study on the structural and electronic properties of AlB$_2$, TiB$_2$ and (Al$_x$, Ti$_{(1-x)}$)B$_2$ in Al–Ti–B master alloys. *J. Alloys Compd.* **585**, 529–534 (2014).

16. X.Z. Li, X.F. Bian, X.J. Li, and X.F. Liu: Ab initio studies of TiB$_2$ and AlB$_2$ in the Al–Ti–B alloy. *Acta Metall. Sin.* **37**, 235–238 (2001).

17. S. Lakshmi, L. Lu, and M. Gupta: *In situ* preparation of TiB$_2$ reinforced Al based composites. *J. Mater. Process. Technol.* **73**, 160–166 (1998).

18. B.S. Murty, S.A. Kori, K. Venkateswarlu, R.R. Bhat, and M. Chakraborty: Manufacture of Al–Ti–B master alloys by the reaction of complex halide salts with molten aluminum. *J. Mater. Process. Technol.* **80**, 152–158 (1999).

19. F. Chen, Z.N. Chen, F. Mao, T.M. Wang, and Z.Q. Gao: TiB$_2$ reinforced aluminum based *in situ* composites fabricated by stir casting. *Mater. Sci. Eng., A* **625**, 357–368 (2015).